Self-assembly of polymer droplets in a nematic liquid crystal at phase separation

Kosuke Kita,* Masatoshi Ichikawa, and Yasuyuki Kimura†
Department of Physics, School of Sciences, Kyushu University, 6-10-1 Hakozaki, Higashi-ku, Fukuoka 812-8581, Japan
(Received 26 November 2007; revised manuscript received 25 December 2007; published 11 April 2008)

We have studied the phase separation of a binary mixture of a polymer and a nematic liquid crystal at a dilute polymer concentration. Various types of regular self-assemblies of polymer droplets such as branched chains and zigzag chains have been observed in addition to the previously reported straight chains. The kinetic process of the self-assembly is dominated by the transformations of a topological defect accompanied by a droplet in addition to the simple growth of the droplet. The spontaneous transformation from a ring defect (Saturn-ring defect) to a point defect (dipole) is an essential process in forming a straight chain composed of droplets with the same size. We also find that the transformations are induced by a nearby droplet with a point defect. This leads to a wide size distribution of droplets in a chain cluster and results in a branched chain. The difference in the chaining mechanisms is discussed using an electrostatic analogy. We also clarify that the symmetry breaking in the assembly is governed by the direction in which the cell containing the binary mixture is rubbed.

DOI: 10.1103/PhysRevE.77.041702 PACS number(s): 61.30.Jf, 82.70.Kj, 47.57.−s

Phase separation in a mixture of simple fluids has been intensively studied from both experimental and theoretical viewpoints [1]. Recently, mixtures of isotropic and anisotropic fluids such as polymers and liquid crystals (LCs) have been actively investigated from fundamental and applicational viewpoints [2,3]. In a polymer-rich system, a polymer-dispersed LC, which is a dispersion of LC droplets in a polymer matrix, has been studied for application to display devices [2]. In a LC-rich system, nematic colloids, which are dispersions of micrometer-sized colloids (or polymers) in a nematic LC solvent, have attracted the attention of researchers as promising starting materials for fabricating mesoscopic structures [4–10]. For example, an anisotropic chain-like structure made of water droplets [4], a linear chain array of silicone oil droplets [5,6], a hexagonal crystal-like structure of glycerol droplets [7], and a two-dimensional crystal comprising silica particles [8] have been realized experimentally. There have also been many theoretical studies on the interaction between colloids and assemblies [11–15].

In a nematic colloid, a colloidal particle with strong surface anchoring deforms the director field of the surrounding LC. The mismatch of the preferred direction of the LC at the particle's surface induces a discontinuous point called a topological defect (or disclination) in the director field [4,10–13]. The topological defect is characterized by the topological charge S, which is determined by the number of times the unit sphere is wound around by all the directors on the surface enclosing the defect core. The defects interact with each other similarly to electric charges through the elastic deformation of the LC [16].

A colloidal particle with a normal anchoring surface in an aligned nematic LC becomes a point defect ($S=+1$) called a radial hedgehog defect, which is accompanied by an additional defect with negative S to minimize the elastic deformation of the LC around the particle. Such colloid-defect pairs interact with each other through the electrostatic analogous force depending on their configuration [11–13,17–19]. There are two typical configurations called a dipole [Fig. 1(a)] and a Saturn ring [Fig. 1(b)]. In the dipolar configuration, a colloidal particle is accompanied by a point defect ($S=-1$) called a hyperbolic hedgehog defect near its pole. This colloid-defect pair behaves as an electric dipole [11,17]. In the Saturn-ring configuration, a colloidal particle is accompanied by a line defect ($S=-1/2$) called a disclination ring around its equator. This pair behaves as an electric quadrupole [11,12].

Recent studies have suggested that the configuration of a colloid-defect pair is qualitatively governed by the size of the colloidal particle. In general, a small particle forms the Saturn-ring configuration and a large one forms the dipolar configuration [8,11–13]. At the phase separation of a polymer-LC mixture in a LC-rich system, polymer droplets coalesce and grow in the nematic host as time elapses. In the early stage, the droplets retain the Saturn-ring configuration and fuse into larger droplets. The Saturn ring transforms into a dipole at a certain critical radius R_c, which is determined by the balance between the surface anchoring energy and the elastic energy [5,6]. Finally, the droplets in the dipolar configuration with radius R_c self-assemble into linear chains along the nematic director by dipolar interactions between them. In the chain clusters, the hyperbolic hedgehog defects

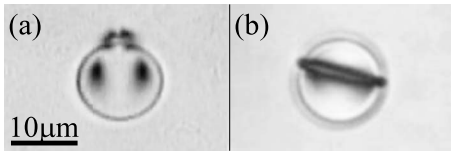

FIG. 1. Polarizing microscopy images of two typical configurations of colloid-defect pair (parallel-Nicoles configuration). The background is nematic LC and the droplets are silicone oil. (a) Dipolar configuration. The singular point at the pole of the droplet is known as a hyperbolic hedgehog defect. (b) Saturn-ring configuration. The black circle surrounding the droplet is a disclination ring.

*k.kita@kyudai.jp
†kimura@phys.kyushu-u.ac.jp

 ©2008 The American Physical Society

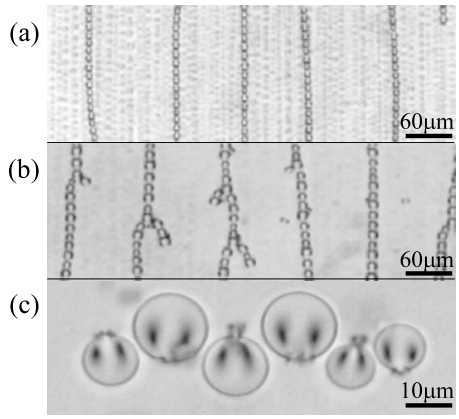

FIG. 2. Chains composed of silicone oil droplets formed by phase separation. (a) Straight chains are formed by quenching to a temperature below room temperature. The sizes of the droplets are almost the same. (b) Branched chains are formed by quenching to room temperature. The chains consist of droplets with various sizes. The branching occurs at larger droplets and its direction is uniform. (c) Zigzag chain composed of dipoles in an antiparallel arrangement.

between the droplets prevent their direct contact and the coalescence of the droplets, as shown in Fig. 2(a). The chains are reported to have two structural features [5,6]. (i) They are composed of uniform-sized droplets. (ii) They are reasonably straight similar to those observed in electro- or magnetorheological fluids under an electric or magnetic field. However, we also found complex regular structures such as branched chains [Fig. 2(b)] and zigzag chains [Fig. 2(c)]. The branching of a chain assembly under different conditions and by different mechanisms has been reported for a nematic LC confined in a capillary [20]. Although the growth process of a straight chain has been reported, the transformation process of the defects and the formation process of the branched and zigzag chains have not been studied yet.

In this paper, we study the fusion and transformation processes of droplet-defect pairs at phase separation in detail. We also discuss the formation mechanism of the self-assemblies formed by the elastic interaction in a nematic LC.

The system studied is a binary mixture of a nematic LC (TL203, Merck, Ltd.) and a silicone oil (viscosity 500, Fluka). The high viscosity of our polymer reduces the rate of phase separation and increases the critical radius R_c. The phase diagram of the mixture is similar to those reported for other polymer-LC mixtures [5]. The mixture exhibits a uniform nematic (N) phase at low concentrations of silicone oil ($\leqslant$4 wt %) around 60 °C. First, we mixed the silicone oil and the LC at the temperature region of the isotropic (Iso) phase of about 70 °C. The mixture in the uniform N phase was injected into a glass cell whose thickness was approximately 20 μm. Both surfaces of the cell were coated with polyvinyl alcohol and rubbed unidirectionally to attain homogeneous alignment in the N phase. The rubbing directions were parallel to each other (parallel rubbing). We quenched the mixture of 2 wt % silicone oil from the N phase (about 60 °C) to the N+Iso phase (about room temperature). We observed the phase separation process under a polarizing microscope (BS-2, Olympus). The images were captured by a charge coupled device camera and recorded on videotapes. Both polarizers were set to the parallel-Nicole configuration, and the defects appeared as dark regions, as shown in Fig. 1.

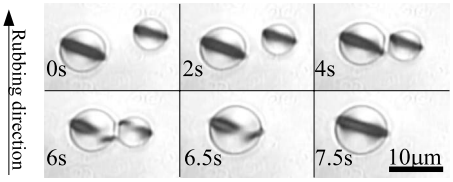

FIG. 3. Fusion of silicone oil droplets in Saturn-ring configuration.

Soon after the quenching, silicone oil droplets were randomly formed in the nematic background. All the observed droplets are accompanied by disclination rings, and their fusion process was observed, as shown in Fig. 3. The two Saturn rings approach obliquely to the rubbing direction by the quadrupolelike interaction. Immediately before the fusion, the rings are pushed aside by the repulsion between them.

After a while, the disclination ring around the equator starts to shrink when it reaches a certain radius R_c, as shown in Fig. 4(a). The shrinking process can be regarded as the transformation from Saturn-ring to dipolar configuration. The direction of shrinkage breaks the up-down symmetry of the nematic LC, and all the dipoles point in the same direction. A similar spontaneous transformation has been reported for the recovery process of an electric-field-induced dipolar configuration by Loudet *et al.* [21]. It takes considerable time for the droplets to transform entirely into the dipolar configuration because of the high viscosity of the polymer. We also found another pathway for the transformation. It can also be induced by a nearby large droplet in the dipolar configuration, as shown in Fig. 4(b). When a Saturn ring is attracted by a nearby dipole, the disclination ring moves due to the attraction of the nearby droplet or the repulsion of a hyperbolic hedgehog defect. By this pathway, droplets whose radii are smaller than R_c can transform into the dipolar configura-

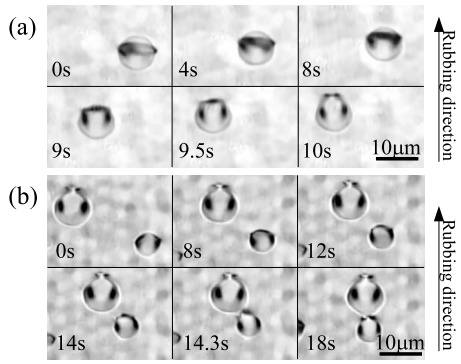

FIG. 4. Process of transformation from Saturn-ring to dipolar configuration. (a) Spontaneous process. The disclination ring continuously shrinks to form the pole of a droplet. The shape of the droplet gradually changes from spherical to ellipsoid. (b) Induced process. The upper-left dipole induces the transformation of the lower-right Saturn ring.

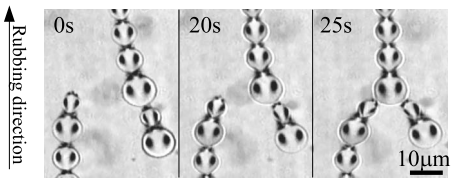

FIG. 5. Branching of an inhomogeneous chain. A hyperbolic hedgehog defect at the end of a chain attaches to a larger droplet. The junction comprises three hyperbolic hedgehog defects around a large droplet.

tion. The droplets in the dipolar configuration formed by this process have various radii smaller than R_c and self-assemble into inhomogeneous chains.

An inhomogeneous short chain grows into a veinlike branched chain, as shown in Fig. 2(b). The typical branching process is shown in Fig. 5. A hyperbolic hedgehog defect accompanying a smaller droplet at the head of a chain slowly approaches a larger droplet in another chain. All the branching points where two dipoles attach to a third dipole consist of a droplet and three surrounding hyperbolic hedgehog defects. The straight chains of the structure are formed under certain conditions. For example, they can be formed by quenching to a lower temperature (deep quenching).

The mechanism of the chaining and branching can be explained by using an electrostatic analogy. The long-range interaction energy between the dipoles labeled 0 and i separated by a separation vector $\boldsymbol{r}$ ($|\boldsymbol{r}|=r$) is given by Lubensky *et al.* [13] as

$$\frac{U(r)}{4\pi K} = p_0 p_i V_{pp}(r) + \frac{2}{3}(c_0 p_i - c_i p_0) V_{pc}(r) + \frac{4}{9} c_0 c_i V_{cc}(r), \tag{1}$$

where K is the elastic constant, p_i ($=2.04a_i$) is the dipole moment, c_i ($=-0.98a_i$) is the quadrupole moment, and a_i is the radius of droplet i. In Eq. (1), V_{pp}, V_{pc}, and V_{cc}, respectively, represent the dipole-dipole interaction $V_{pp}=(1-3\cos^2\theta)/r^3$, the dipole-quadrupole interaction $V_{pc}=(15\cos^3\theta-9\cos\theta)/r^4$, and the quadrupole-quadrupole interaction $V_{cc}=(9-90\cos^2\theta+105\cos^4\theta)/r^5$, where θ is the angle between $\boldsymbol{r}$ and the far-field director. The second term is asymmetric in the direction of the nematic director, and its sign depends on the relative positions of a large and small dipole. However, this term can be neglected when dipoles have a uniform size ($a_i=a_0$). We calculated the interaction energy between dipole 0 and a chain composed of dipoles labeled $i=1,\ldots,21$, as shown in Fig. 6. We also plot the unit force vector as black arrows in Fig. 6.

First, we considered the condition under which all the Saturn rings transform through the spontaneous process. The chain is composed of droplets with the same size ($a_{i=1,\ldots,21}=R_c$). We set the test dipole 0 ($a_0=R_c$) near this homogeneous chain, as shown in Fig. 6(a). The potential profile and force field around the chain are also shown in Fig. 6(a). It is clear that the test dipole is able to approach the chain from the direction of its head and tail. Straight chains are formed under such an experimental condition when the transformation is mainly governed by the spontaneous process.

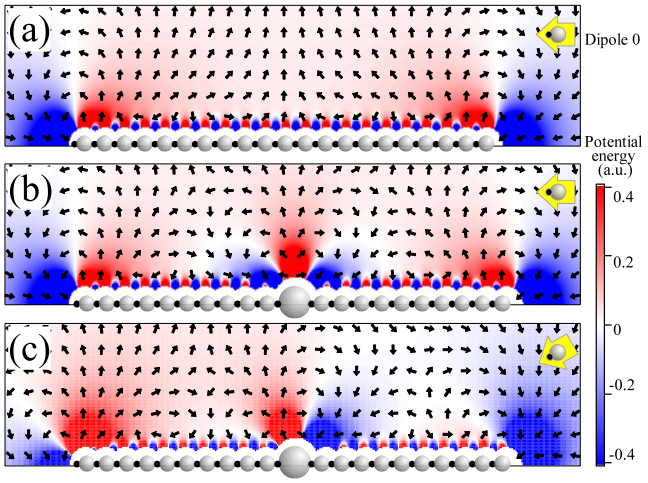

FIG. 6. (Color online) Interaction potential profile between a test dipole 0 and a chain composed of 21 dipoles. Negative potentials indicate the attractive region and positive ones indicate the repulsive region. Black arrows indicate the unit force vector. (a) Dipole 0 ($a_0=R_c$) around a homogeneous chain ($a_{i=1,\ldots,21}=R_c$). (b) Dipole 0 ($a_0=R_c/2$) around an inhomogeneous chain ($a_{i\neq 11}=R_c/2$, $a_{11}=R_c$). (c) Dipole 0 is set at an angle of 30° to the far-field director in the vicinity of the inhomogeneous chain shown in (b).

Second, we consider the condition under which almost all the Saturn rings transform through the induced process. The chain is composed of droplets with $a_{i\neq 11}=R_c/2$ and $a_{11}=R_c$. We set the dipole 0 ($a_0=R_c/2$) around this inhomogeneous chain. The potential profile and the force field around such an inhomogeneous chain are shown in Fig. 6(b). Two additional attractive regions appear around the dipole 11. Dipole 0 can approach the chain while still far from the chain, and the chain can branch in four preferential directions around the large droplet. The branch to the right-hand side of the chain is composed of three hyperbolic hedgehog defects around a droplet, and the branch to the left-hand side is composed of three droplets around a hyperbolic hedgehog defect. The bilateral symmetry of the potential indicates that the second term in $U(r)$ does not effect the branching.

The force profile in Fig. 6(b) appears to be accurate when the dipole is a long distance from the chain. However, at a sufficiently short distance, as shown in Fig. 5, the direction of the defect accompanying the dipole is slightly tilted from the rubbing direction toward the larger droplet. The effect of the inclination of the approaching dipole is calculated by simply setting dipole 0 at a fixed angle of 30° to the far-field director [Fig. 6(c)]. We neglect the quadrupole moments in the calculation because they have little effect on the branching process. In this case, one attractive region near the large droplet expands, and this results in unidirectional branching.

We also elucidated the origin of asymmetry in the defect transformation using a cell for which the half of the inner surface is rubbed upward and half is rubbed downward, as shown in Fig. 7(a). We can experimentally confirm that the branching direction is determined by the rubbing direction [Fig. 7(b)]. It is significant that LC molecules are inclined slightly upward from the cell surface toward the rubbing di-

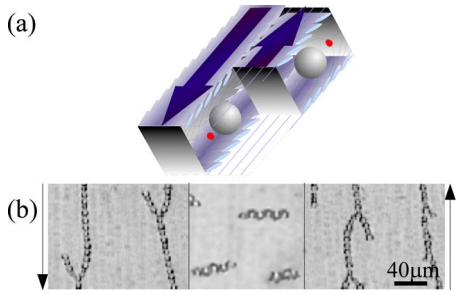

FIG. 7. (Color online) Branching direction determined by the rubbing direction. The left part of a cell is rubbed downward and the right part is rubbed upward (parallel rubbing). The directions of rubbing are indicated by black arrows. (a) Schematics of the director field near a droplet. (b) Polarizing microscope images of the chains observed.

rection. The director field near the cell surfaces uniquely determines the direction of the dipole by the asymmetry of the director field around the dipole. In particular, the dipoles are arranged in an antiparallel direction in the middle of the cell. They can point both upward and downward because of the overlap of the rubbing directions. Such a zigzag chain has been reported as one of the stable arrangements that can be built using optical tweezers [8,17].

In conclusion, we have studied the kinetic process of the phase separation in a mixture of a polymer and a nematic LC. The characteristic interactions between colloidal particles in the nematic LC enable the formation of various types of assemblies. The transformations of a droplet-defect pair through the spontaneous and induced processes have been directly observed. The size polydispersity in a chain cluster caused by the induced process causes the branching. This type of induced process is dominant when the critical radius for the spontaneous process becomes larger with increasing polymer viscosity, concentration of silicone oil, and temperature after quenching. In addition, the rubbing direction governs the symmetry breaking during the defect transformation.

This study was financially supported by a Grant-in-Aid for Scientific Research from JSPS and a Grant-in-Aid for Scientific Research on Priority Area "Soft Matter Physics" from MEXT, Japan.

[1] A. Onuki, *Phase Transition Dynamics* (Cambridge University Press, Cambridge, England, 2002).
[2] P. S. Drzaic, *Liquid Crystal Dispersions* (World Scientific, Singapore, 1995).
[3] R. G. Larson, *The Structure and Rheology of Complex Fluids* (Oxford University Press, New York, 1999).
[4] P. Poulin, H. Stark, T. C. Lubensky, and D. A. Weitz, Science **275**, 1770 (1997).
[5] J. C. Loudet, P. Barois, and P. Poulin, Nature (London) **407**, 611 (2000).
[6] J. C. Loudet, P. Barois, P. Auroy, H. Richard, and P. Poulin, Langmuir **20**, 11336 (2004).
[7] V. G. Nazarenko, A. B. Nych, and B. I. Lev, Phys. Rev. Lett. **87**, 075504 (2001).
[8] I. Muševič, M. Škarabot, U. Tkalec, M. Ravnic, and S. Žumer, Science **313**, 954 (2006).
[9] M. Zapotocky, L. Ramos, P. Poulin, T. C. Lubensky, and D. A. Weitz, Science **283**, 209 (1999).
[10] P. Poulin and D. A. Weitz, Phys. Rev. E **57**, 626 (1998).
[11] H. Stark, Phys. Rep. **351**, 387 (2001).
[12] E. M. Terentjev, Phys. Rev. E **51**, 1330 (1995).
[13] T. C. Lubensky, D. Pettey, N. Currier, and H. Stark, Phys. Rev. E **57**, 610 (1998).
[14] T. Araki and H. Tanaka, Phys. Rev. Lett. **97**, 127801 (2006).
[15] J. Fukuda and H. Yokoyama, Eur. Phys. J. E **4**, 389 (2001).
[16] P. M. Chaikin and T. C. Lubensky, *Principles of Condensed Matter Physics* (Cambridge University Press, Cambridge, England, 1998).
[17] M. Yada, J. Yamamoto, and H. Yokoyama, Phys. Rev. Lett. **92**, 185501 (2004).
[18] I. I. Smalyukh, O. D. Lavrentovich, A. N. Kuzmin, A. V. Kachynski, and P. N. Prasad, Phys. Rev. Lett. **95**, 157801 (2005).
[19] C. M. Noël, G. Bossis, A.-M. Chaze, F. Giulieri, and S. Lacis, Phys. Rev. Lett. **96**, 217801 (2006).
[20] P. Kossyrev, M. Ravnik, and S. Zumer, Phys. Rev. Lett. **96**, 048301 (2006).
[21] J. C. Loudet, O. Mondain-Monval, and P. Poulin, Eur. Phys. J. E **7**, 205 (2002).